

# UC Irvine

## UC Irvine Previously Published Works

### Title

Quantifying nuclear wide chromatin compaction by phasor analysis of histone Förster resonance energy transfer (FRET) in frequency domain fluorescence lifetime imaging microscopy (FLIM) data.

### Permalink

<https://escholarship.org/uc/item/99w8j52t>

### Authors

Liang, Zhen  
Lou, Jieqiong  
Scipioni, Lorenzo  
et al.

### Publication Date

2020-06-01

### DOI

10.1016/j.dib.2020.105401

Peer reviewed



## Data Article

# Quantifying nuclear wide chromatin compaction by phasor analysis of histone Förster resonance energy transfer (FRET) in frequency domain fluorescence lifetime imaging microscopy (FLIM) data

Zhen Liang<sup>a,b</sup>, Jieqiong Lou<sup>a,b</sup>, Lorenzo Scipioni<sup>c</sup>, Enrico Gratton<sup>c</sup>, Elizabeth Hinde<sup>a,b,\*</sup>

<sup>a</sup> School of Physics, University of Melbourne, Australia

<sup>b</sup> Department of Biochemistry and Molecular Biology, Bio21 Institute, University of Melbourne, Australia

<sup>c</sup> Department of Biomedical Engineering, Laboratory for Fluorescence Dynamics, University of California, Irvine, United States

## ARTICLE INFO

## Article history:

Received 6 February 2020

Revised 3 March 2020

Accepted 3 March 2020

Available online 12 March 2020

## Keywords:

Förster resonance energy transfer

Fluorescence lifetime imaging microscopy

Phasor analysis

Histone

Chromatin compaction

Nuclear architecture

## ABSTRACT

The nanometer spacing between nucleosomes throughout global chromatin organisation modulates local DNA template access, and through continuous dynamic rearrangements, regulates genome function [1]. However, given that nucleosome packaging occurs on a spatial scale well below the diffraction limit, real time observation of chromatin structure in live cells by optical microscopy has proved technically difficult, despite recent advances in live cell super resolution imaging [2]. One alternative solution to quantify chromatin structure in a living cell at the level of nucleosome proximity is to measure and spatially map Förster resonance energy transfer (FRET) between fluorescently labelled histones – the core protein of a nucleosome [3]. In recent work we established that the phasor approach to fluorescence lifetime imaging microscopy (FLIM) is a robust method for the detection of histone FRET which can quantify nuclear wide chromatin compaction in the presence of cellular autofluorescence [4]. Here we share FLIM data recording histone

\* Corresponding author at: School of Physics, University of Melbourne, Australia.

E-mail address: [elizabeth.hinde@unimelb.edu.au](mailto:elizabeth.hinde@unimelb.edu.au) (E. Hinde).

FRET in live cells co-expressing H2B-eGFP and H2B-mCherry. The data was acquired in the frequency domain [5] and processed by the phasor approach to lifetime analysis [6]. The data can be valuable to researchers interested in using the histone FRET assay since it highlights the impact of cellular autofluorescence and acceptor-donor ratio on quantifying chromatin compaction. The data is related to the research article “Phasor histone FLIM-FRET microscopy quantifies spatiotemporal rearrangement of chromatin architecture during the DNA damage response” [4].

© 2020 Published by Elsevier Inc.

This is an open access article under the CC BY-NC-ND license. (<http://creativecommons.org/licenses/by-nc-nd/4.0/>)

Specifications table

Subject	Biophysics
Specific subject area	Fluorescence lifetime imaging microscopy (FLIM) of Förster resonance energy transfer (FRET) between fluorescently labelled histones.
Type of data	Frequency domain FLIM data (.R64 files) acquired in live human cell nuclei co-expressing a histone FRET pair (H2B-eGFP and H2B-mCherry). The R64 file format contains in each pixel the corrected G versus S coordinate describing the donor fluorescence lifetime and the local donor intensity. The R64 file format can be directly opened and analysed in the software SimFCS developed at the Laboratory for Fluorescence Dynamics or imported into Matlab as a matrix via the provided Matlab script ‘Open_R64.m’. We also provide a Matlab script called ‘Phasor_FRET.m’ that extrapolates the FRET trajectory for a given unquenched donor and background phasor.
How data were acquired	FLIM data were acquired on an Olympus FV3000 laser scanning confocal microscope coupled to a pulsed 488 nm laser operated at 80 MHz and an ISS FastFLIM box for time resolved detection via the digital frequency domain (DFD) method. The ISS Vista vision software was used for instrument calibration as well as data acquisition and the SimFCS software was used for phasor transformation and data analysis.
Data format	Raw and graph
Parameters for data collection	The FLIM data were acquired in the donor channel (H2B-eGFP) since the fluorescence lifetime of the donor reports FRET interaction with the acceptor (H2B-mCherry) – our read out of nuclear wide chromatin compaction.
Description of data collection	The ISS FastFLIM box was first pre-calibrated against a fluorescence lifetime standard so that the saved FLIM acquisitions of histone FRET (.R64 files) are corrected and ready for phasor-based lifetime analysis (e.g., in SimFCS or Matlab).
Data source location	School of Physics, University of Melbourne, Melbourne, Australia.
Data accessibility	The raw data files (.R64), Matlab code to open .R64 files (Open_R64.m) and script to extrapolate a specific donor-background phasor FRET trajectory (Phasor_FRET.m) are provided in the Data in Brief Dataverse, <a href="https://dataverse.harvard.edu/privateurl.xhtml?token=317d358d-2d23-466f-af12-b2b15c284c9c">https://dataverse.harvard.edu/privateurl.xhtml?token=317d358d-2d23-466f-af12-b2b15c284c9c</a>
Related research article	All other data is with this article. Jieqiong Lou, Lorenzo Scipioni, Belinda K. Wright, Tara K. Bartolec, Jessie Zhang, V. Pragathi Masamsetti, Katharina Gaus, Enrico Gratton, Anthony J. Cesare, and Elizabeth Hinde. 2019. Phasor histone FLIM-FRET microscopy quantifies spatiotemporal rearrangement of chromatin architecture during the DNA damage response’.

Value of the data

- The fluorescence lifetime imaging microscopy (FLIM) data presented here demonstrate how to detect Förster resonance energy transfer (FRET) between fluorescently labelled histones and how this signal can be used as a readout of chromatin compaction in live cells.

- The FLIM data presented will benefit researchers interested in establishing the histone FRET assay in their specific cell system and the FLIM data shared will serve as a resource for learning the phasor approach to histone FRET analysis of chromatin compaction.
- The data can be used as a guide for researchers optimising histone FRET sample preparation (e.g., acceptor-donor ratio) and provide insight into how to quantify histone FRET by phasor analysis in the presence of cellular autofluorescence.

## 1. Data Description

The fluorescence lifetime imaging microscopy (FLIM) data presented in Fig. 1 were acquired in live U2OS cells expressing H2B-eGFP (donor) in the absence (raw .R64 files titled *H2BGFP\_CELL1-3* and *H2BGFP\_FREEMCH\_CELL1-3*) and presence of an increasing amount of H2B-mCherry (acceptor) (raw .R64 files titled *H2BGFP\_EQUAL\_H2BMCH\_CELL1-3* and *H2BGFP\_EXCESS\_H2BMCH\_CELL1-3*) via use of an Olympus FV3000 laser scanning confocal microscope coupled to a pulsed 488 nm laser operated at 80 MHz and an ISS FastFLIM box for time resolved detection in the frequency domain (workflow behind histone FLIM-FRET experiment described in Experimental Design, Materials and Methods). The aim of this FLIM data is to demonstrate how detection of Förster resonance energy transfer (FRET) between fluorescently labelled histones in a living cell can report nuclear wide chromatin compaction at the level of nucleosome proximity via the phasor approach to fluorescence lifetime analysis (theory behind phasor transformation of FLIM-FRET data described in Experimental Design, Materials and Methods).

In a H2B-eGFP and H2B-mCherry FRET experiment the fluorescence lifetime of H2B-eGFP (donor) reports the efficiency of interaction with H2B-mCherry (acceptor) over a spatial scale of 1–10 nm in each pixel of a diffraction limited FLIM image. Thus, while intensity data are acquired in both the H2B-eGFP and H2B-mCherry channels to verify co-expression of the FRET pair (Fig. 1(a) and (b)), FLIM data only needs to be acquired in the H2B-eGFP channel to spatially map FRET efficiency – our readout of the nanometre spacing between nucleosomes throughout global chromatin architecture (Fig. 1(c)). FLIM data were quantified in terms of FRET efficiency by the phasor approach to lifetime analysis, which transforms the fluorescence lifetime of H2B-eGFP recorded in each pixel of a FLIM image into a two-dimensional coordinate system termed a phasor plot (Fig. 1(d)). In the phasor plot, independent mixtures of fluorophores can be distinguished from changes in lifetime due to FRET, thus enabling quantitation of the different chromatin states throughout a nucleus in the presence of background cellular autofluorescence. From comparison of histone FRET in U2OS cells expressing a fixed window of low H2B-eGFP expression with a low versus high window of H2B-mCherry expression we demonstrate the acceptor-donor ratio to be an important consideration in a histone FRET experiment (Fig. 1(e)). In particular we find that the acceptor (H2B-mCherry) should be present in an equal to excess amount of the donor (H2B-eGFP) to promote the probability of histone FRET being a possible outcome between adjacent nucleosomes and to limit the unquenched donor from dominating the histone FRET signal. However, since there is an inversely proportional relationship between acceptor-donor ratio and the baseline of inter-nucleosome FRET for a specific window of co-expression, it is important that only cells with a similar acceptor-donor ratio are compared, or if possible, a sorted stable cell line is generated.

Next in Fig. 2 we manipulate higher order chromatin structure to demonstrate that histone FRET is sensitive to rearrangement in chromatin compaction for a specific window of co-expression (i.e., acceptor-donor ratio). Specifically, we present intensity (Fig. 2(a)) and FLIM data (Fig. 2(b)) where live U2OS cells expressing H2B-eGFP (donor) in the absence (raw .R64 files titled *H2BGFP\_CELL1-3*) and presence of H2B-mCherry (acceptor) (raw .R64 files titled *H2BGFP\_H2BMCH\_CELL1-3*) were subjected to a hypotonic (raw .R64 files titled *H2BGFP\_H2BMCH\_HYPO\_CELL1-3*) versus hypertonic (raw .R64 files titled *H2BGFP\_H2BMCH\_HYPER\_CELL1-3*) treatment that opens and compacts the chromatin network, respectively [7]. This data demonstrates that histone FRET for a given baseline of inter-

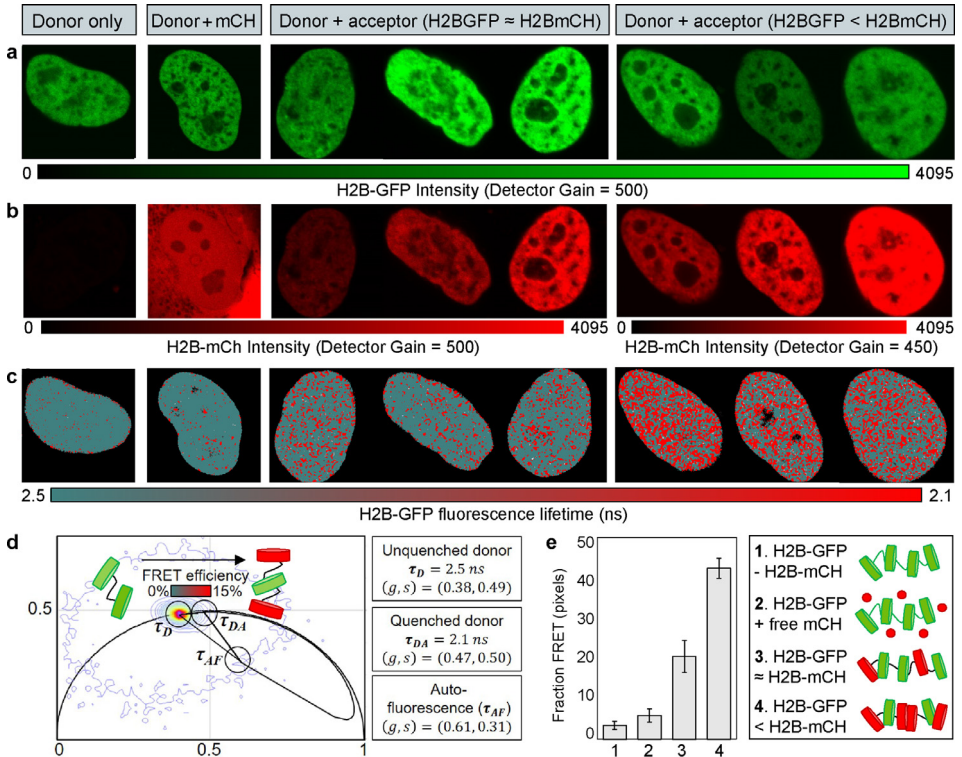


**Fig. 1.** Phasor analysis of histone FRET in frequency domain FLIM data reports chromatin compaction with a baseline sensitivity determined by the underlying acceptor-donor ratio. (a)–(b) Intensity images acquired in the donor (eGFP) (a) versus acceptor (mCherry) (b) channel of live U2OS cells expressing: (1) H2B-eGFP in the absence of H2B-mCherry (unquenched donor control, raw data .R64 files titled *H2BGFP\_CELL1-3*), (2) H2B-eGFP in the presence of free mCherry (bleed through control, raw data .R64 files titled *H2BGFP\_FREEMCH\_CELL1-3*), (3) H2B-eGFP in the presence of H2B-mCherry (FRET experiment with acceptor/donor ratio  $\approx 1$ , raw data .R64 files titled *H2BGFP\_EQUAL\_H2BMCH\_CELL1-3*) and (4) H2B-eGFP in the presence of an excess of H2B-mCherry (FRET experiment with acceptor/donor ratio  $\approx 2$ –3, raw data .R64 files titled *H2BGFP\_EXCESS\_H2BMCH\_CELL1-3*). (c) FLIM images acquired in the donor channel (eGFP) of the U2OS cell experiments presented in (a)–(b) pseudo-colored according to a palette that reports FRET (i.e., extends from the unquenched donor phasor (teal) to the quenched donor phasor (red)) (d) The FRET palette is derived from the combined phasor distribution of H2B-eGFP in the absence versus presence of H2B-mCherry. The theoretical FRET trajectory superimposed enables the range of FRET efficiencies present in the different acceptor-donor ratio samples presented to be spatially mapped and quantified. Note that the phasor location of background autofluorescence was measured in plain U2OS cells (raw data .R64 files titled *BACKGROUND\_AF\_CELL1-3*) and the theory behind the FRET trajectory is described in the Experimental Design, Materials and Method section. (e) Quantitation of the number of pixels in each FLIM image undergoing FRET (i.e., reporting high chromatin compaction) reveal the acceptor-donor ratio to impact the baseline FRET efficiency of a histone FRET experiment. Error bars represent SEM for  $N = 3$  cells in panel (e). (For interpretation of the references to colour in this figure legend, the reader is referred to the web version of this article.)

nucleosomal FRET (acceptor-donor ratio  $\approx 1$ –2) directly reports chromatin compaction (i.e., palette extending from unquenched donor phasor to FRET state coincides with the phasor of open versus compacted chromatin) (Fig. 2(c)) and serves as an accurate readout of nuclear wide chromatin condensation (Fig. 2(d)). Importantly, the hypotonic versus hypertonic induced rearrangements in chromatin compaction have minimal impact on the fluorescence lifetime of H2B-eGFP in the absence of H2B-mCherry (Fig. 2(e)) and thus these two chemical treatments (outlined in the Experimental Design, Materials and Methods section) serve as a valuable tool for FLIM based evaluation of histone FRET in a specific cell line or biological system and the dynamic range of chromatin compaction states that can be accessed for a given window of donor-acceptor co-expression.

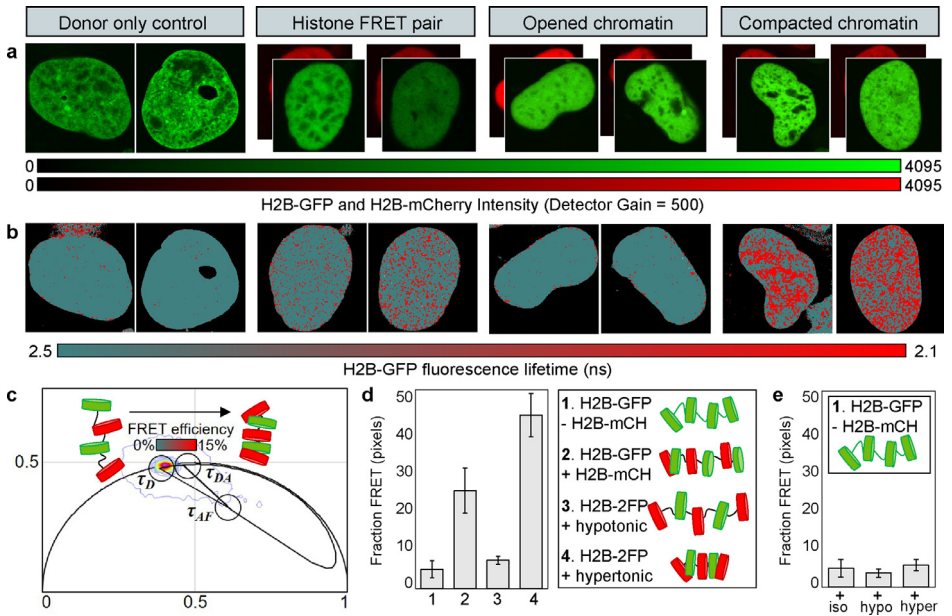


**Fig. 2.** Phasor analysis of histone FRET in frequency domain FLIM data is sensitive to drug induced changes in nuclear wide chromatin compaction. (a) Intensity images acquired in the donor (eGFP) and acceptor (mCherry) channel of live U2OS cells expressing: (1) H2B-eGFP in the absence of H2B-mCherry (unquenched donor control, raw data .R64 files titled *H2BGFP\_CELL1-3*), (2) H2B-eGFP in the presence of H2B-mCherry (histone FRET experiment, raw data .R64 files titled *H2BGFP\_H2BMCH\_CELL1-3*), (3) H2B-eGFP in the presence of H2B-mCherry after hypotonic treatment (open chromatin histone FRET experiment, raw data .R64 files titled *H2BGFP\_H2BMCH\_HYPO\_CELL1-3*) and (4) H2B-eGFP in the presence of H2B-mCherry after hypertonic treatment (compact chromatin histone FRET experiment, raw data .R64 files titled *H2BGFP\_H2BMCH\_HYPER\_CELL1-3*). (b) FLIM images acquired in the donor channel (eGFP) of the U2OS cell experiments presented in (a) pseudo-colored according to a palette that reports FRET, and as shown via hypotonic versus hypertonic induced changes in chromatin structure, directly reports chromatin compaction (i.e., the unquenched donor phasor (teal) coincides with open chromatin and the FRET state (red) coincides with compaction chromatin). (c) The FRET palette is derived from the combined phasor distribution of H2B-eGFP in the absence versus presence of H2B-mCherry, before and after hypotonic versus hypertonic treatment (as outlined in Experimental Design, Materials and Methods). The theoretical FRET trajectory superimposed enables the range of FRET efficiencies reporting different chromatin compaction states to be spatially mapped and quantified. (d) Quantitation of the number of pixels in each FLIM image undergoing FRET in response hypotonic opening versus hypertonic compacting of chromatin demonstrates histone FRET as a sensitive read out of nuclear wide chromatin condensation. Note H2B-2FP represents H2B-eGFP + H2B-mCh. (e) Hypotonic versus hypertonic opening and compacting of the chromatin network does not significantly impact the fluorescence lifetime of H2B-eGFP and thus these controls treatments serve as a valuable tool to evaluate FLIM based analysis of histone FRET in a specific cell line expressing a specific donor-acceptor ratio. Error bars represent SEM for  $N = 3$  cells in panel (d)-(e). (For interpretation of the references to colour in this figure legend, the reader is referred to the web version of this article.)

## 2. Experimental Design, Materials and Methods

### 2.1. Fluorescence lifetime imaging microscopy (FLIM) of histone FRET in live cells

Fluorescence lifetime imaging microscopy (FLIM) can be performed in the frequency or time domain (as described extensively elsewhere [8,9]) and phasor-based histone FRET analysis is compatible with both types of acquisition [6,10,11]. Here live cell FLIM was performed on an Olympus FV3000 laser scanning microscope coupled to a 488 nm pulsed laser operated at 80 MHz and an ISS A320 FastFLIM box for time resolved detection that is based on the digital frequency domain (DFD) method [5]. A 60X water immersion objective 1.2 NA was used for all experiments and the cells were imaged at 37 degrees in 5% CO<sub>2</sub>. In terms of sample preparation, U2OS cells were grown in DMEM (Lonza) supplemented with 10% bovine growth serum (Gibco),



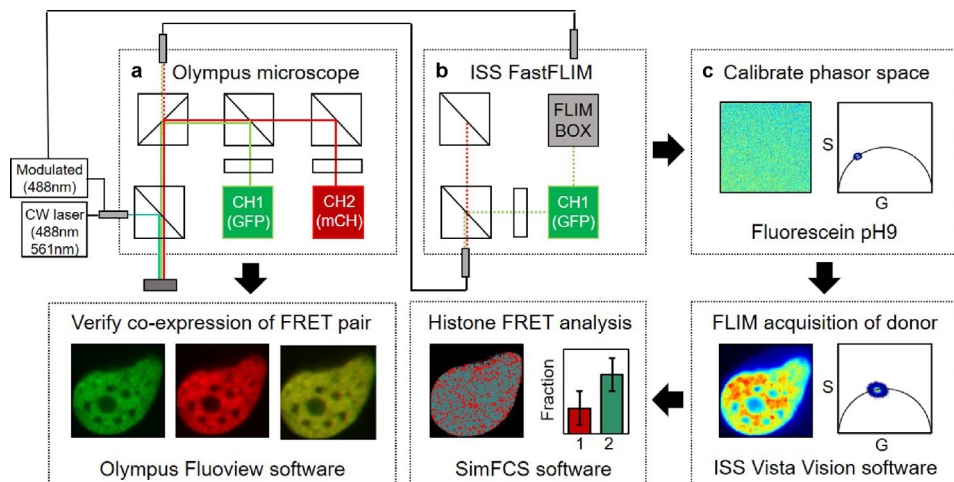


**Fig. 3.** Workflow behind a histone FLIM-FRET experiment performed on the Olympus confocal scanning microscope that is coupled to an ISS FastFLIM box for time resolved detection. (a) To find a U2OS cell nucleus co-expressing H2B-eGFP and H2B-mCh at a specific acceptor-donor ratio we first set up a light path within the Olympus FV3000 confocal laser scanning microscope that employed the internal continuous wave lasers and GaAsP PMTs to detect eGFP and mCherry signal (top panel), and then used the Olympus Fluoview software to acquire a two-channel intensity image of a selected nucleus co-expressing the histone FRET pair (bottom panel). (b) To acquire a FLIM image of histone FRET within the selected U2OS cell nucleus we modified the Olympus FV3000 light path set up to employ an external modulated 488 nm laser source (80MHz) and then directed *only* the donor fluorescence (eGFP signal) to the external ISS FastFLIM box for time resolved detection. (c) Prior to FLIM acquisition of histone FRET experiments we calibrated the ISS FastFLIM system and phasor space by measurement of fluorescein at pH 9 (top panel) and then in the ISS Vista Vision software applied the derived phase versus modulation corrections to all subsequent FLIM acquisitions of donor fluorescence (H2B-eGFP) performed on the same day (bottom right panel). The fluorescence lifetime of H2B-eGFP recorded in each pixel of a FLIM image was then transformed into histone FRET by phasor analysis in the SimFCS software, which enabled chromatin compaction to be spatially mapped and quantified (bottom left panel).

1 x Pen-Strep (Lonza) and 1  $\mu\text{g/ml}$  puromycin (Thermo Fisher Scientific) at 37°C in 5%  $\text{CO}_2$ . The U2OS cells were then plated 24 h before a FLIM experiment onto 35 mm glass bottom dishes and transiently transfected with the following plasmids via use of Lipofectamine 3000 according to the manufacturer's protocol: (1) H2B-eGFP (donor control), (2) H2B-eGFP and H2B-mCherry (FRET experiment) and (3) H2B-eGFP and free mCherry (negative FRET control). To manipulate higher order chromatin structure and demonstrate histone FRET is sensitive to rearrangement in chromatin compaction, U2OS cells expressing the donor control versus FRET experiment were subjected to two different types of osmotic shock that open and compact chromatin [7]. To open chromatin via hypotonic shock, imaging medium was diluted with distilled water until reaching a ratio of 35:65 v/v, and to compact chromatin via hypertonic shock, imaging medium was supplemented with 160 mM sucrose.

Although equal amounts of DNA were used to co-transfect U2OS cells with the histone FRET pair, significant heterogeneity in terms of eGFP versus mCherry co-expression was observed at the single cell level and this heterogeneity needs to be taken into account when quantifying a baseline for histone FRET in a specific cell system. Thus, intensity images ( $512 \times 512$  pixel frame size, 20  $\mu\text{s/pixel}$ , 45 nm/pixel) of H2B-eGFP versus H2B-mCherry within selected U2OS nuclei were first acquired in sequential mode to verify co-expression of transfected plasmids and determine the acceptor-donor ratio via use of internal solid-state laser diodes operating at 488 nm and 561 nm, respectively (Fig. 3(a)). The resulting fluorescence signal was then directed through a 405/488/561 dichroic mirror to remove laser light and the eGFP versus mCherry emission detected by two internal GaAsP photomultiplier detectors set to collect the following bandwidths: 500–550 nm and 600–650 nm. All intensity images of H2B-eGFP were acquired with a fixed laser power as well as detector gain setting (500 V) and then compared to intensity images of

H2B-mCh acquired with a fixed laser power and two different detector gain settings (500 V versus 450 V). This acquisition enabled U2OS cells to be selected for histone FRET analysis that had a low versus high acceptor-donor ratio (as detailed in Fig. 1).

A FLIM image (256 × 256 pixel frame size, 20 μs/pixel, 90 nm/pixel, 20 frame integration) was then acquired within the same U2OS nucleus and field of view in only the H2B-eGFP channel for subsequent FRET analysis, via use of the external pulsed 488 nm laser (80 MHz) (Fig. 3(b)). The resulting fluorescence signal was directed through a 405/488/561 dichroic mirror to remove laser light and a 550 nm long pass filter to split the donor signal from any direct excitation of the acceptor. The remaining donor signal was then collected by an external photomultiplier detector (H7422P-40 of Hamamatsu) fitted with a 520/50 nm bandwidth filter and processed by the ISS A320 FastFLIM box data acquisition card that employs the digital frequency domain (DFD) technique to report the fluorescence lifetime of H2B-eGFP recorded in each pixel. The FLIM data were acquired by the ISS Vista Vision software that pre-calibrates the instrument and phasor space against a known reference lifetime (we use fluorescein at pH 9 which has a known single exponential lifetime of 4.04ns) (Fig. 3(c)). Here we provide the resulting calibrated files (.R64 format) that can be opened and directly analysed in the software SimFCS developed at the Laboratory for Fluorescence Dynamics (LFD) as well as a script labelled 'Open\_R64.m' that enables the .R64 files to be opened in Matlab and processed by alternative phasor based codes. The '.R64' files contain the corrected g and s coordinates derived in each pixel of the FLIM image – the parameters that describe fluorescence lifetime – as well as the local intensity.

## 2.2. Phasor analysis of FLIM data acquired in the frequency domain and calculation of the FRET trajectory

The phasor method of lifetime analysis is “native” to the DFD method of FLIM data acquisition [5] and the .R64 files we provide to demonstrate histone FRET analysis. In the instance researchers wish to analyse the .R64 files via a custom made script in Matlab here we first provide the theory behind phasor transformation of DFD FLIM data (Fig. 4(a)–(c)) and phasor analysis of linear combinations versus histone FRET (Fig. 4(d)–(h)). In the instance researchers wish to analyse the .R64 files directly in SimFCS we demonstrate in the next section (text describing Fig. 5) the steps taken to generate Figs. 1 and 2 and quantitation of chromatin compaction [4]. Frequency domain lifetime methods are characterised by the usage of a periodic modulated excitation (Fig. 4(a)) for which the finite lifetime of the fluorophore results in a phase delay ( $\phi$ ) and a demodulated emission (m) (Fig. 4(b)) [5]. In the ISS Vista Vision software these intensity normalised characteristics of the fluorescence lifetime recorded in each pixel of a FLIM image are transformed into their instrument corrected cosine (G) and sine (S) components according to:

$$\begin{cases} G_{i,j}(\omega) = m_{i,j} \cos(\phi_{i,j}) \\ S_{i,j}(\omega) = m_{i,j} \sin(\phi_{i,j}) \end{cases} \quad (1)$$

where  $m_{i,j}$  versus  $\phi_{i,j}$  are the modulation and the phase delay of emission at the pixel indexes  $i$  and  $j$  with respect to the excitation that has a laser repetition angular frequency of  $\omega = 2\pi f$  [6]. The G and S coordinate recorded in each pixel of a FLIM image is then plotted in a two-dimensional histogram called a phasor plot (Fig. 4(c)), that when used in reciprocal mode, enables each point of the phasor plot to be mapped to each pixel of the FLIM image [10]. Since phasors follow simple vector algebra, it is possible to determine the fractional contribution of two or more independent molecular species coexisting in the same pixel (Fig. 4(d)). For example, in the case of two independent species (e.g., autofluorescence and H2B-eGFP) all possible weightings give a phasor distribution along a linear trajectory that joins the phasors of the individual species in pure form according to:

$$\begin{cases} G_{i,j}(\omega) = \sum_n f_n \cdot g_{i,j,n}(\omega) \\ S_{i,j}(\omega) = \sum_n f_n \cdot s_{i,j,n}(\omega) \end{cases} \quad (2)$$



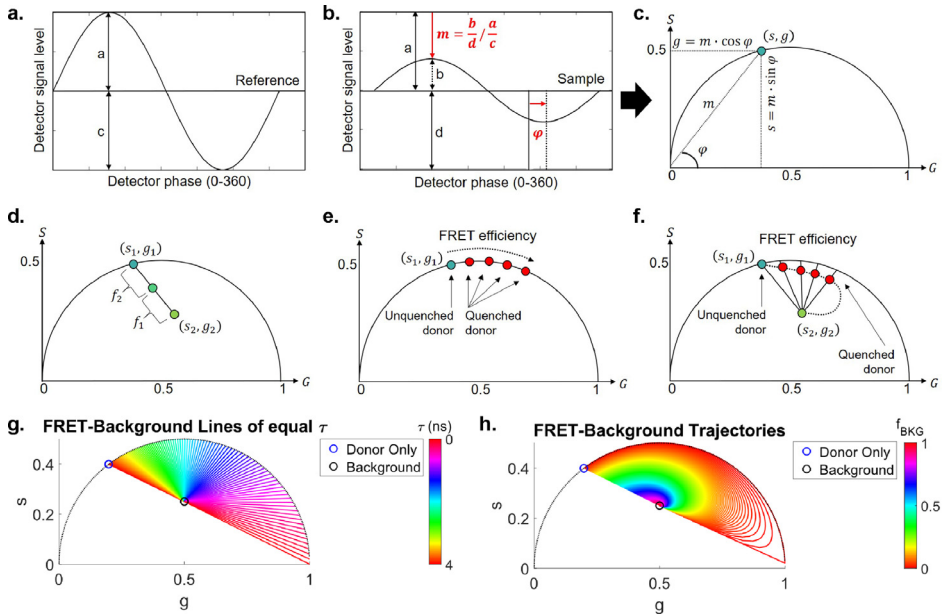


**Fig. 4.** Theory behind phasor transformation of frequency domain FLIM data and phasor analysis of FRET in the presence of cellular autofluorescence. (a)-(b) In frequency domain FLIM the fluorescence lifetime of a sample is determined by exciting a sample with a modulated light source (a) and measuring the sample's emission, which has the same frequency but is demodulated ( $m$ ) and phase-shifted ( $\phi$ ) with respect to the excitation source (b). (c) The demodulation ( $m$ ) and phase shift ( $\phi$ ) of the fluorescent emission report the sample's fluorescence lifetime ( $\tau$ ) and this property can be graphically represented as a vector by the phasor approach to lifetime analysis. (d) The advantage of phasor-based lifetime analysis is that phasors follow simple vector algebra and thus it is possible to determine the fractional contribution of two or more independent molecular species coexisting in the same pixel (i.e., the contribution of species 1 is  $f_1 / f_1 + f_2$ ). (e)-(f) In the case of FRET, where a donor molecule's lifetime is quenched upon interaction with an acceptor molecule, a phasor shift will be observed that follows a FRET trajectory defined by Eq. (6) in the absence of background (e) and Eq. (15) in the presence of background (f). In the latter case the FRET trajectory will be pulled inside the universal circle as a result of forming a linear combination with additional species (e.g., cellular autofluorescence). (g) The unquenched donor to background phasor linear combination from which a FRET trajectory would be extrapolated calculated for a range of single exponential lifetimes. (h) The FRET trajectory of a given single exponential donor in the presence of increasing background. Panel (g)-(h) were generated by the Matlab script Phasor\_FRET.m

where  $f_n$  are the fractional fluorescence intensities of each phasor component such that  $\sum_n f_n = 1$ . In the case of a single exponential lifetime  $m_{i,j} = \cos \phi_{i,j}$ . This corresponds to a point in a semi-circle on the phasor plot called the “universal circle” which is given by:

$$S_{i,j}^2 + \left(G_{i,j} - \frac{1}{2}\right)^2 = \frac{1}{4} \quad (3)$$

In the case of a FRET experiment, where the lifetime of the donor molecule is quenched upon interaction with an acceptor molecule (e.g., H2B-eGFP interaction with H2B-mCh), the FRET trajectory is defined as the realisation of all possible phasors ( $G, S$ ) the donor lifetime can adopt as a function of the FRET efficiency  $E_{FRET}$ , in the absence (Fig. 4(e)) or presence (Fig. 4(f)) of a background signal such as autofluorescence [11]. These calculations require the phasor position of the unquenched donor ( $G_d, S_d$ ) and background ( $G_{bkg}, S_{bkg}$ ) to be obtained from calibration experiments. Starting from the background-free case, the FRET efficiency is calculated from:

$$E_{FRET} = 1 - \frac{\tau_{da}}{\tau_d} \quad (4)$$

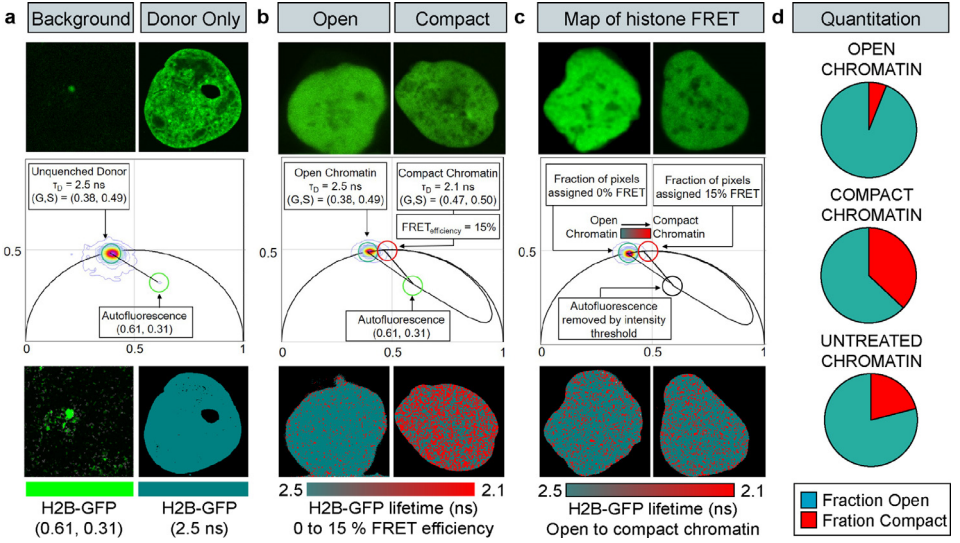


**Fig. 5.** Phasor based histone FRET analysis in practice and quantification of nuclear wide chromatin network compaction. (a) Phasor analysis of a plain U2OS nucleus (background) versus a U2OS nucleus expressing H2B-eGFP (donor only) enables identification of the linear combination of phasor coordinates from which the histone FRET trajectory should be extrapolated. (b) Phasor analysis of a U2OS nucleus expressing the histone FRET pair (H2B-eGFP + H2B-mCherry) after hypotonic versus hypertonic treatment and superimposition of a FRET trajectory based on the calibration in (a) enables identification of the phasor coordinates of open versus compact chromatin to coincide with the donor only control at 2.5 ns and a 15% FRET efficiency at 2.1 ns. (c) Phasor analysis of untreated U2OS nuclei expressing the histone FRET pair (H2B-eGFP + H2B-mCherry) enables the different chromatin compaction states to be spatially mapped by application of a histone FRET palette that extends from the open to compact chromatin phasor. Cellular autofluorescence was removed via application of an intensity threshold ( $\approx 20$  counts). (d) The nuclear wide chromatin network compaction status of a U2OS cell expressing the histone FRET pair can be calculated under different conditions and across multiple cells when the fraction of pixels highlighted by the open versus compact cursor are quantified ( $N=3$  cells).

where  $\tau_d$  is the single exponential lifetime of the unquenched donor and  $\tau_{da}$  is the quenched lifetime of the donor, which given  $\tau_{da} = (1 - E_{FRET}) \cdot \tau_d$  and  $\tau_d$  is a pure exponential, then  $\tau_{da}$  will also lie on the universal circle. The phasor coordinates of  $\tau_{da}$  are analytically defined by:

$$\begin{cases} G_{da} = \frac{1}{1 + \omega^2 \tau_{da}^2} \\ S_{da} = \frac{\omega \tau_{da}}{1 + \omega^2 \tau_{da}^2} \end{cases} \quad (5)$$

where  $\omega = 2\pi f$  and  $f$  is in Hz. The FRET trajectory in the background-free case is ultimately defined as:

$$\begin{cases} G_{da}(E_{FRET}) = \frac{1}{1 + ((1 - E_{FRET}) \cdot \omega \tau_d)^2} \\ S_{da}(E_{FRET}) = \frac{(1 - E_{FRET}) \cdot \omega \tau_d}{1 + ((1 - E_{FRET}) \cdot \omega \tau_d)^2} \end{cases} \quad (6)$$

The addition of background will affect the  $(G, S)$  position of the phasor by pulling the result inside the universal circle. In the case of the unquenched donor, the new position will be defined by:

$$\begin{cases} G_{d,bkg} = G_d \cdot f_d + G_{bkg} \cdot f_{bkg} \\ S_{d,bkg} = S_d \cdot f_d + S_{bkg} \cdot f_{bkg} \end{cases} \quad (7)$$

where  $f_d$  and  $f_{bkg}$  are the relative photon contribution from the unquenched donor and the background, respectively. These parameters can be calculated from the intensity of the unquenched

donor,  $I_d$  and the background  $I_{bkg}$  which are defined by:

$$\begin{cases} f_d = \frac{I_d}{I_d + I_{bkg}} \\ f_{bkg} = \frac{I_{bkg}}{I_d + I_{bkg}} \\ f_d + f_{bkg} = 1 \end{cases} \quad (8)$$

If FRET occurs, less photons will be emitted from the quenched donor, therefore the intensity  $I_{da}$  will be reduced and the contribution of the background will be increased. Specifically, the FRET efficiency can also be defined by:

$$E_{FRET} = 1 - \frac{I_{da}}{I_d} \quad (9)$$

and therefore:

$$I_{da} = (1 - E_{FRET}) \cdot I_d \quad (10)$$

Inverting Eq. (8) we can obtain  $I_d$  as a function of  $f_d$  and  $I_{bkg}$ :

$$I_d = \frac{I_{bkg}}{f_d^{-1} - 1} \quad (11)$$

The same inversion can be applied for  $I_{da}$  and substituted into Eq. (10) to obtain:

$$\frac{I_{bkg}}{f_{da}^{-1} - 1} = (1 - E_{FRET}) \cdot \frac{I_{bkg}}{f_d^{-1} - 1} \quad (12)$$

Rewritten as:

$$f_{da}(E_{FRET}) = \frac{1}{1 + \frac{f_d^{-1} - 1}{1 - E_{FRET}}} \quad (13)$$

From which the background fraction is simply:

$$f_{bkg}(E_{FRET}) = 1 - f_{da}(E_{FRET}) \quad (14)$$

And the trajectory becomes:

$$\begin{cases} G_{da,bkg}(E_{FRET}) = G_{da}(E_{FRET}) \cdot f_{da}(E_{FRET}) + G_{bkg} \cdot f_{bkg}(E_{FRET}) \\ S_{da,bkg}(E_{FRET}) = S_{da}(E_{FRET}) \cdot f_{da}(E_{FRET}) + S_{bkg} \cdot f_{bkg}(E_{FRET}) \end{cases} \quad (15)$$

where  $G_{da}(E_{FRET})$  and  $S_{da}(E_{FRET})$  are the same computed for the background-free case in Eq. (6) and  $f_{da}(E_{FRET})$  and  $f_{bkg}(E_{FRET})$  come from Eqs. (13) and (14), respectively. To visually demonstrate the implications of Eq. (15) on calculation of the FRET trajectory in Fig. 4(g) we show the unquenched donor-background phasor linear combination from which a FRET trajectory can be extrapolated for a range of single exponential lifetimes and in Fig. 4(h) the FRET trajectory of a specific donor lifetime in the presence of increasing background. The extension of this analytical concept to multi-exponential lifetimes is computed under the assumption that FRET equally affects each exponential present.

### 2.3. Phasor analysis of histone FRET and quantification of nuclear wide chromatin compaction

With the theory behind phasor transformation of frequency domain FLIM data and calculation of a FRET trajectory in mind, here we now present how in practice to quantify histone FRET and spatially map chromatin compaction within a FLIM image (e.g., Figs. 1 and 2). The phasor coordinates of the unquenched donor and cellular autofluorescence from which the FRET trajectory is extrapolated, are first calibrated independently in live U2OS cells that are un-transfected versus transfected with H2B-eGFP (Fig. 5(a)). Colored cursors are then assigned to these two terminal phasor locations (i.e., teal cursor centered at 2.1 ns for unquenched donor and green

cursor for autofluorescence) to enable these two phasor distributions to be mapped to each pixel of the FLIM image. Next the dynamic range of FRET efficiencies describing chromatin network organisation in our biological system is determined by measurement of the phasor coordinates that correspond to 'open' versus 'compact' chromatin in live U2OS cells transfected with the histone FRET pair (H2B-eGFP and H2B-mCherry) and subjected to hypotonic versus hypertonic treatment, respectively (Fig. 5(b)). As can be seen in Fig. 5(b): (1) open chromatin coincides with the phasor location of the unquenched donor (teal cursor centered at 2.5 ns), (2) compact chromatin is right shifted to a shorter lifetime (new red cursor centered at 2.1 ns), and (3) from superimposition of a FRET trajectory defined by our unquenched donor-background calibration over the combined phasor distribution of 'open' versus 'compact' chromatin, U2OS cells exhibit chromatin compaction states with nucleosome proximities that range from 0 to 15% in FRET efficiency. Finally, by linking the teal and red cursors centered at 'open' versus 'compact' chromatin we generate a palette that reports the chromatin condensation status in each pixel of a H2B-eGFP FLIM map derived in untreated U2OS cells expressing the histone FRET pair (Fig. 5(c)). The fraction of pixels within any one condensation state of interest can be calculated per nucleus and this enables quantification of nuclear wide chromatin network organisation across multiple cells (Fig. 5(d)). It is important to note that in the one photon excitation experiments (488 nm diode operating at 80 MHz) presented in this manuscript the background autofluorescence in U2OS cells was minimal and this signal could be removed via application of an intensity threshold ( $\approx 20$  counts). However in experiments where background autofluorescence is more significant or comparable to the histone FRET signal being investigated, the cursor between the donor phasor and cellular autofluorescence should also be linked so that the contribution of background can be quantified in each pixel [4]. It is also important to note that the hypotonic versus hypertonic treatments were found to have negligible impact on the fluorescence lifetime of the donor (H2B-eGFP) and therefore not cause artefact in quantification of histone FRET when the acceptor (H2B-mCherry) is present. In contrast, some drug treatments (e.g., Actinomycin D) do induce a subtle shift in the donor lifetime and the impact this has on detection of histone FRET needs to be quantified, to determine a baseline for detection of chromatin compaction events in the presence of the acceptor (H2B-mCherry) [4]. For all of the FLIM data presented here a  $3 \times 3$  spatial median filter was applied to the FLIM maps prior to FRET analysis and all quantitation was performed in the SimFCS software developed at the LFD.

## Acknowledgments

This work was supported by an [Australian Research Council](#) (ARC) discovery project (DP180101387), a [National Health and Medical Research Council](#) (NHMRC) project grant (APP1104461) and U.S. National Institute of Health grants (P41-GM103540 and P50-GM076516). EH is supported by an [NHMRC](#) Career Development Fellowship (APP1124762) and the Jacob Haimson Beverly Mecklenburg Lectureship. Imaging was performed within the Biological Optical Microscopy Platform, University of Melbourne.

## Conflict of Interest

The authors declare that they have no known competing financial interests or personal relationships that could have appeared to influence the work reported in this paper.

## References

- [1] B. Bonev, G. Cavalli, Organization and function of the 3D genome, *Nat. Rev. Genet.* 17 (12) (2016) 772.
- [2] H.D. Ou, et al., ChromEMT: visualizing 3D chromatin structure and compaction in interphase and mitotic cells, *Science* 357 (6349) (2017) 357–370.

- [3] D. Lleres, et al., Quantitative analysis of chromatin compaction in living cells using FLIM-FRET, *J. Cell Biol.* 187 (4) (2009) 481–496.
- [4] J. Lou, et al., Phasor histone FLIM-FRET microscopy quantifies spatiotemporal rearrangement of chromatin architecture during the DNA damage response, *Proc. Natl. Acad. Sci. U. S. A.* 116 (15) (2019) 7323–7332.
- [5] R.A. Colyer, C. Lee, E. Gratton, A novel fluorescence lifetime imaging system that optimizes photon efficiency, *Microsc. Res. Tech.* 71 (3) (2008) 201–213.
- [6] M.A. Digman, et al., The phasor approach to fluorescence lifetime imaging analysis, *Biophys. J.* 94 (2) (2008) L14–L16.
- [7] A. Walter, et al., Crowded chromatin is not sufficient for heterochromatin formation and not required for its maintenance, *J. Struct. Biol.* 184 (3) (2013) 445–453.
- [8] R.M. Clegg, O. Holub, C. Gohlke, Fluorescence lifetime-resolved imaging: measuring lifetimes in an image, *Methods Enzymol.* 360 (2003) 509–542.
- [9] C.Y. Dong, et al., Fluorescence-lifetime imaging techniques for microscopy, *Methods Cell Biol.* 72 (2003) 431–464.
- [10] S. Ranjit, et al., Fit-free analysis of fluorescence lifetime imaging data using the phasor approach, *Nat. Protoc.* 13 (9) (2018) 1979–2004.
- [11] E. Hinde, et al., Biosensor Forster resonance energy transfer detection by the phasor approach to fluorescence lifetime imaging microscopy, *Microsc. Res. Tech.* 75 (3) (2012) 271–281.